Basic research

Rheumatology

Exosomes derived from bone marrow mesenchymal stem cells pre-treated with curcumin alleviate osteoporosis by promoting osteogenic differentiation via regulating the METTL3/microRNA-320/RUNX2 signaling pathway

Yunhui Zhang*

Department of Orthopedics, Baoshan Hospital, Shanghai, China

Submitted: 24 May 2020; **Accepted:** 28 July 2020
Online publication: 18 April 2021

Arch Med Sci 2026; 22 (3): 1822–1837
DOI: https://doi.org/10.5114/aoms/125788

***Corresponding author:**
Yunhui Zhang
Department of Orthopedics
Baoshan Hospital
29 Tuanjie Rd.
Shanghai, China, 201999
E-mail: boneresearch@126.com

Abstract

Introduction: Curcumin (CUR) has been reported to stimulate the expression of methyltransferase-like 3 (METTL3), a potential therapeutic target for osteoporosis. Also, bone marrow mesenchymal stem cell (BMSC)-derived exosomes (EXO) have been demonstrated to improve osteoporosis by pro-moting the proliferation of osteoblasts. In this study, we aimed to study the effect of CUR and BMSC-derived exosomes in the treatment of osteoporosis.
Material and methods: Microscopy was used to characterize exosomes derived from BMSCs. MicroCT was carried out to analyze the parameters of bone formation. Western blot was carried out to analyze the expression of surface markers on BMSC-derived exosomes and METTL3/Runt-related transcription factor 2 (RUNX2) proteins under different conditions. Realtime PCR was used to assess the gene expression under different circumstances.
Results: The exosomes derived from CUR-treated BMSCs showed an enhanced therapeutic effect on osteoporotic mice compared with exosomes derived from untreated BMSCs. Mechanistically, CUR pretreatment of BMMSCs significantly enhanced the ability of BM-MSCderived exosomes to restore the dysregulated expression of METTL3, miR-320, and RUNX2. Addi-tionally, CUR treatment of BMSCs markedly enhanced the stimulatory effect of BMSC-derived exosomes on the expression of METTL3, miR-320, RUNX2, BGLAP, and LAP in BMSCs. Furthermore, luciferase assay demonstrated that miR-320 was capable of suppressing the expression of RUNX2 through bind-ing to the 3' UTR of RUNX2.
Conclusions: Our study demonstrated that BMSC-derived exosomes could modulate the METTL3/miRNA-320/RUNX2 axis to attenuate osteoporosis by promoting osteogenic differentiation of BMSCs. Moreover, the CUR treatment of BMSCs promoted the therapeutic effect of BMSC-derived exosomes.

Key words: osteoporosis, curcumin, exosome, bone marrow stem cells, methyltransferase-like 3, miRNA-320, runt-related transcription factor 2.

Introduction

As a bone condition characterized by reduced bone mass, damaged bone microstructure, decreased bone strength, and increased bone fragility, osteoporosis increases the risk of fractures. The risk of osteoporosis in-

creases with age [1, 2]. Along with the aging of the population worldwide, osteoporosis has become one of the most costly illnesses worldwide [3]. Osteoporosis can be classified into two types: primary and secondary osteoporosis.

A yellow polyphenolic substance derived from the extract of *Curcuma longa* (curcumin – CUR), has been shown to possess anti-tumor, anti-inflammatory, anti-oxidant, and anti-bacterial properties [4, 5]. Specifically, CUR was demonstrated to exhibit its anti-inflammatory effect via promoting the production of interleukin-10 (IL-10) and thus accordingly enhancing pathological interactions mediated by IL-10 [6]. Previous studies have shown that CUR may impair the function of tissue factors related to thrombotic diseases by inhibiting the aggregation of platelets or by decreasing platelet activity [7]. In addition, many studies have found that CUR exerts a beneficial effect in alleviating osteoporosis in both clinical and experimental models [8]. Previous research indicated that the combined administration of CUR and alendronate could enhance bone mineral density (BMD) and modulate bone turnover markers in postmenopausal women with osteoporosis [9]. Also, unlike all-trans retinoic acid (ATRA), which inhibited the mineralization of differentiated cells during the later stages, CUR was proved to increase the osteogenic differentiation capacity of bone marrow stem cells (BMSCs) [10]. Moreover, the pre-administration of CUR into the BMSCs could facilitate cell therapy in tissue repair treatment by improving mitochondrial function and destabilizing HIF-1α, leading to the obstruction of potential hypoxia/reoxygenation injury [11, 12]. It was found that CUR prevented LPS-induced augmentation of SCD-1 and SREBP-1c mRNA expression in the liver. Especially, CUR in the diet impacts METTL14, METTL3, FTO, ALKBH5, and YTHDF2 mRNA expression while increasing the content of m6A in piglet liver [13].

BMSC are reported to release exosomes containing the molecules of over 150 types of different miRNAs [14]. Numerous studies have revealed that exosomes play a primary role in the therapeutic functions of BMSCs. In the cardiovascular system, medium conditioned by BMSCs improved heart functions [15]. Other studies found that mice treated with BMSC-derived exosomes showed a reduced size of cardiac infarct *ex vivo* as well as *in vivo* [14, 16, 17]. BMSC exosomes derived from rats, humans, and mice have shown curative effects in a range of various diseases [18]. It was also shown that hFOB 1.19 cell proliferation was enhanced by mesenchymal stem cell (MSC)-derived exosomes, thus alleviating osteoporosis [19].

METTL3 was initially recognized as a primary methyltransferase in the process of methylation and was later verified to exert an effect on the progression of certain cancers [20, 21]. It was found that the METTL3 deletion in MSCs interrupts the normal cell cycle in mice, leading to osteoporosis. In addition, the gain-of-function of METTL3 protects against postmenopausal osteoporosis induced by estrogen deficiency [22]. Another study found that the methylation of pre-miR-320 mediated by METTL3 promoted bone formation as well as the osteogenic differentiation of BMSCs [23]. It was reported that by acting as a pro-osteogenic or an anti-osteoporotic factor, METTL3 could maintain a high level of RUNX2 expression via direct methylation of RUNX2 as well as indirect upregulation of RUNX2 expression through pre-miR-320 methylation [23]. Also, RUNX2, as previously reported, acts as a transcription factor specific to osteoblasts which plays a critical role in the differentiation of MSCs into osteoblasts [24, 25]. RUNX2 could regulate osteoblast differentiation by triggering the expression of several major bone matrix genes during the early stages of osteoblast differentiation [24].

Overexpression of METTL3 has been reported as a potential approach to replacement therapy for the treatment of osteoporosis [23]. Moreover, it was also demonstrated that CUR affected the expression of METTL3 in the pathogenesis of LPS-induced liver injury [13]. Moreover, MSC-derived exosomes were proven to improve osteoporosis by promoting the proliferation of osteoblasts [19]. It has been shown that encapsulation within exosomes improves the delivery of curcumin [26]. On the other hand, combination with curcumin enhances the therapeutic effect of exosomes [27]. Based on the above-mentioned evidence, we hypothesized that curcumin may promote expression of METTL3, which will subsequently downregulates expression of miR-320 by hypermethylation of the promoter region, and, as a result, the expression of RUNX3, a direct target gene of miR-320, could be upregulated. Furthermore, pretreatment with CUR will enhance the therapeutic effect of BMSC-derived exosomes in the treatment of osteoporosis. To test the hypothesis, we studied the effect of CUR and BMSC-derived exosomes in rat and cellular models of osteoporosis. Expression of METTL3, miR-320, and RUNX2 was investigated *in vivo* and *in vitro* to identify the signaling pathway underlying the therapeutic effect of CUR on osteoporosis.

Material and methods

Animals and treatment

C57BL/6 mice with an average age of 8 weeks old were acquired from our animal center. All mice were kept in a specific pathogen-free (SPF) environment in the animal facility of our institu-

tion. All animal experiments in this study were approved by the Institutional Animal Care and Use Committee and were conducted in strict compliance with the Guide for the Care and Use of Laboratory Animals published by the US National Institutes of Health (NIH). After 7 days of adaptation, the mice were divided into 4 groups: 1. Sham group (mice undergoing sham operation); 2. Osteoporosis group (mice induced with osteoporosis); 3. Osteoporosis + EXO group (mice induced with osteoporosis and then treated with EXO extracted from untreated BMSCs); and 4. Osteoporosis + EXO-CUR group (mice induced with osteoporosis and then treated with EXO extracted from BMSCs treated with CUR).

Mouse model of osteoporosis

C57BL/6 mice with an average age of 8 weeks were used to create the osteoporosis model. In brief, the model mice were subject to bilateral ovariectomy by exposing the bilateral ovaries and removing nearby adipose tissues. The mice in the sham group also underwent the ovariectomy operation without removing tissues. After the operation, all mice in the groups were kept alive for 8 weeks before being killed to harvest tissue samples for subsequent analyses. The animals in each group were evaluated by microCT.

Primary cell extraction and culture

In this study, BMSCs were isolated from femur and tibia bones collected from Sprague Dawley (SD) rats under aseptic conditions. In brief, before the collection of tibia and femur bones, the rats were killed via cervical vertebra dislocation. Then, BMSCs were isolated via rinsing the cavity of bone marrow with Modified Eagle Medium (MEM, Gibco, Rockville, MD) containing a higher glucose content. Subsequently, the collected BMSCs were cultured in Dulbecco's Modified Eagle Medium (DMEM, Gibco, Rockville, MD) supplemented with 10% fetal bovine serum, 1% penicillin–streptomycin, and 1% L-glutamine (HyClone, South Logan, UT). The culture conditions were 37°C, 5% CO_2 and saturated humidity. After the confluence of BMSCs reached 80%, they were trypsinized (Beyotime, Shanghai, China) for sub-culture. BMSCs between passages 2-5 were used for further analyses. In the EXO-CUR group, the BMSCs were incubated with CUR (1 μM) for 24 h before the isolation of EXO.

Exosome extraction

To remove the residual cells, the cell supernatants of BMSCs were collected and centrifuged at 300 g for 10 min and 2000 g for 15 min at 4°C. To remove the cell debris, a subsequent centrifugation at 12,000 g for 30 min at 4°C was conducted. Particles larger than 200 nm were removed by 0.22 μm filtration. The cell suspensions were centrifuged at 100,000 g for 2 h at 4°C again before the cell supernatants were discarded. For the final re-suspension step, PBS buffer was applied before preservation at –80°C.

RNA isolation and real-time PCR

In this study, real-time PCR was used to assay the relative expression of METTL3, miR-320, RUNX2 mRNA, BGLAP mRNA, and TOUR mRNA in each sample. In brief, the collected tissue and cell samples were lysed using Trizol reagent (Invitrogen, Carlsbad, CA) in accordance with the manufacturer's instructions to isolate total RNA, which was then converted to cDNA using a cDNA RT assay kit (TAKARA, Tokyo, Japan) in accordance with the manufacturer's instructions. In the next step, the cDNA was used as the template for real-time PCR reactions, which were performed using a SYBR Premix EX Taq assay kit (TARKARA, Tokyo, Japan) on a PRISM 7900HT real-time PCR system (ABI, Foster City, CA) in accordance with the manufacturer's instructions. Finally, the relative expression of METTL3, miR-320, RUNX2 mRNA, BGLAP mRNA, and TOUR mRNA in each sample was calculated using the $2^{-\Delta\Delta Ct}$ method.

Cell culture and transfection

BMSCs and MG63 cells were bought from ATCC and cultured in DMEM under conditions suggested by the manufacturer. Then, after the cell confluence reached 80%, the cells were divided into 3 groups, i.e., 1. NC group (cells treated with PBS only); 2. CUR group (cells treated with CUR); and 3. EXO-CUR group (cells treated with CUR-carrying EXO). Then, the cells were treated under corresponding conditions for 48 h before the cells were harvested for target gene analysis. Similarly, BMSCs and MG63 cells were divided into 2 groups, i.e., 1. NC siRNA group (cells treated with a scramble control siRNA); 2. METTL3 siRNA group (cells treated with METTL3 siRNA), and the target gene analysis was done after the cells were transfected with corresponding siRNAs for 48 h using Lipofectamine 2000 (Invitrogen, Carlsbad, CA) in accordance with the manufacturer's instructions.

Vector construction, mutagenesis, and luciferase assay

Our binding site screening found that miR-320 could potentially bind to the 3' UTR of RUNX2. Therefore, to clarify the regulatory relationship between the expression of miR-320 and RUNX2, luciferase vectors containing wild type and mu-

tant RUNX2 were established. First, the wild type 3' UTR of RUNX2 containing the miR-320 binding site was amplified and cloned into a pcDNA3.1 vector (Promega, Madison, WI) downstream of the luciferase gene to create the wild type vector for the 3' UTR of RUNX2. At the same time, mutagenesis was carried out to generate one site-directed mutation in the miR-320 binding site located in the 3' UTR of RUNX2, and the mutant fragment of 3' UTR of RUNX2 was also amplified and cloned into another pcDNA3.1 vector to generate the mutant type vector for the 3' UTR of RUNX2. In the next step, BMSCs and MG63 were co-transfected with mutant type/wild type vectors for the 3' UTR of RUNX2 together with miR-320 mimics or a control using Lipofectamine 2000, and the luciferase activity of transfected cells was measured at 48 h after the start of co-transfection with a Dual-luciferase assay kit (Promega, Madison, WI) on a luminometer in accordance with the manufacturer's instructions.

Western blot analysis

Cell and tissue samples were first lysed using a RIPA lysis system (Beyotime, Shanghai, China) in accordance with the manufacturer's instructions. Then, 20 µg of proteins from each sample were fractionated by using a 10% SDS-PAGE gel, and the fractionated proteins were electro-transferred onto a polyvinylidene fluoride membrane (Millipore, Burlington, MA), which was blocked by using 5% non-fat, washed with TBST, and treated overnight (4°C) with anti-METTL3 and anti-RUNX2 primary antibodies (Abcam, Cambridge, MA) in accordance with the manufacturer's instructions, followed by further incubation against HRP-conjugated secondary antibodies (Santa Cruz Biotechnology, Santa Cruz, CA) at ambient temperature for 2 h. Finally, the protein bands were developed using an enhanced chemiluminescence reagent (Thermo Scientific, Waltham, MA) in accordance with the manufacturer's instructions, and the relative expression of METTL3 and RUNX2 proteins in each sample was semi-quantified using a Chemi-Doc XRS+ machine (Bio-Rad laboratories, Hercules, CA) and the ImageJ 1.40 software.

Immunohistochemistry

For immunofluorescence assays, the samples were made into 4 µm thick slides and blocked with 5% BSA for 1 h before they were incubated successively with anti-METTL3 primary antibodies, and suitable Alexa Fluor 568-conjugated secondary antibodies (all antibodies were obtained from Abcam, Cambridge, MA and used in accordance with the manufacturer's instructions). After counterstaining with DAPI, the positive expression of METTL3 protein in each sample was evaluated under an Axio Observer Z1 microscope coupled with a Zeiss LSM 5 imaging system (Carl Zeiss, Oberkochen, Germany).

Statistical analysis

All data analyses were conducted using GraphPad Prism 6.0 software (GraphPad, San Diego, CA). Two-tailed Student's *t*-tests were used for the comparison between two groups. All data were presented as mean ± standard deviation (SD), and each observation was repeated in triplicate. *P*-values < 0.05 were considered statistically significant.

Results

Isolation and characterization of BMSC-derived exosomes

BMSCs were cultured for 3 days, and their morphology exhibited a vortex distribution and a spindle-like shape under a microscope (Figure 1 A). Exosomes were isolated from BMSCs and the shape of exosomes was evaluated using electron microscopy; the results showed exosomes as round bubbles with a 40 nm diameter (Figure 1 B). Furthermore, Western blot was carried out to analyze the expression of CD9, CD63, and CD81 in the supernatant of BMSCs as well as in BMSC-derived exosomes. The expression of CD9, CD63, and CD81 was significantly elevated in BMSC-derived exosomes when compared with that in the supernatant of BMSCs (data not shown).

CUR treatment markedly enhanced the therapeutic effect of BMSC-derived exosomes in mice with osteoporosis

In order to evaluate the therapeutic effect of CUR on BMSC-derived exosomes, a mouse model of osteoporosis was established. MicroCT was used to measure the bone volume/tissue volume ratio (BV/TV), BMD, trabecular number (Tb.N), trabecular thickness (Tb.Th), and trabecular separation (Tb.Sp) of the osteoporotic mice treated with different therapeutic strategies. Accordingly, the BV/TV, BMD, Tb.N and Tb.Th were remarkably decreased in osteoporotic mice, while BMSC-derived exosomes exerted a notable effect on restoring the values of BV/TV, BMD, Tb.N, and Tb.Th in osteoporotic mice. Moreover, exosomes derived from CUR-treated BMSCs more significantly increased BV/TV (Figures 2 A, F), BMD (Figures 2 B, F), Tb.N (Figures 2 C, F), and Tb.Th (Figures 2 D, F) in osteoporotic mice. In contrast, CUR treatment clearly enhanced the effect of BMSC-derived exosomes on suppressing the abnormally increased Tb.Sp value in osteoporotic mice (Figures 2 E, F).

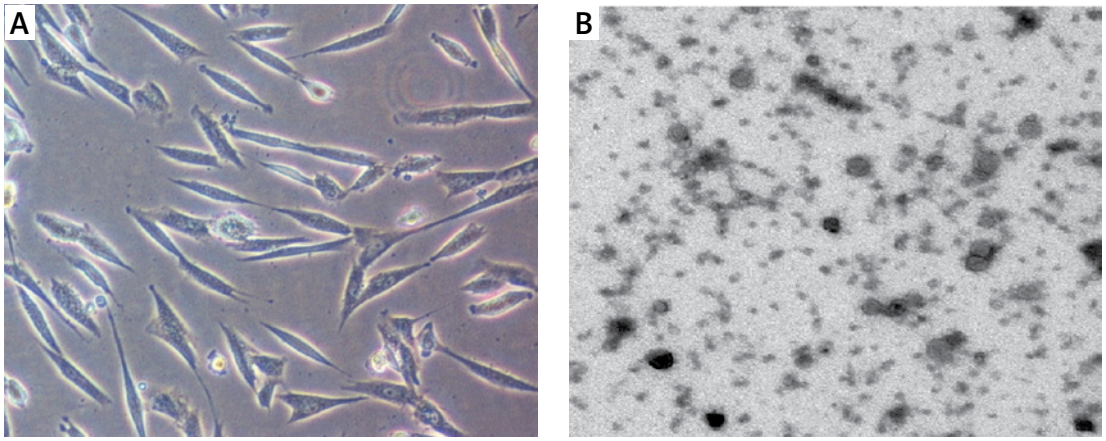

Figure 1. Characterization of exosomes isolated from bone marrow stem cells. **A** – Primary bone marrow stem cells exhibited elongated, spindle-shaped morphology. **B** – Representative images of BMSC-derived exosomes observed under an electron microscope

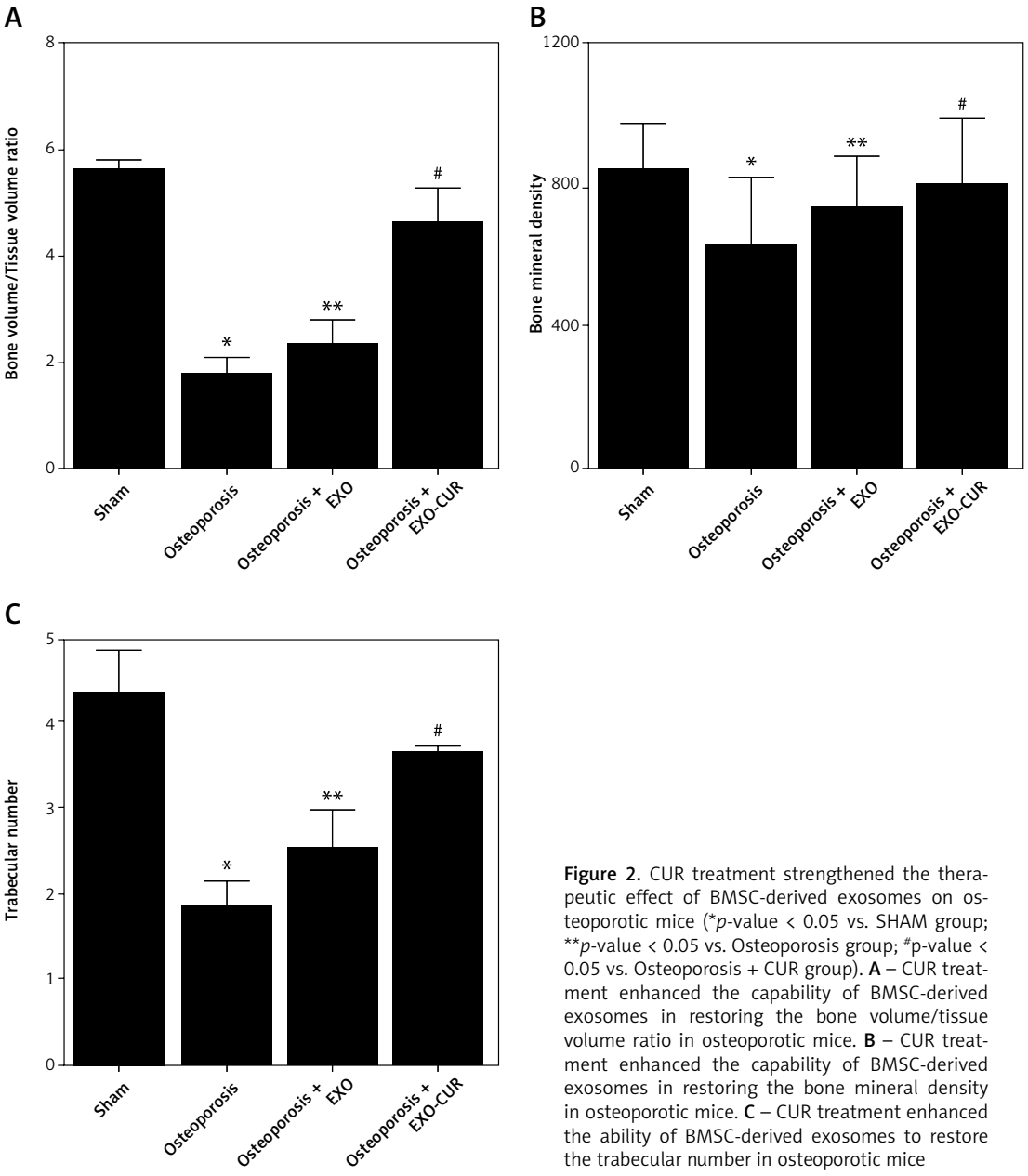

Figure 2. CUR treatment strengthened the therapeutic effect of BMSC-derived exosomes on osteoporotic mice (**p*-value < 0.05 vs. SHAM group; ***p*-value < 0.05 vs. Osteoporosis group; #p-value < 0.05 vs. Osteoporosis + CUR group). **A** – CUR treatment enhanced the capability of BMSC-derived exosomes in restoring the bone volume/tissue volume ratio in osteoporotic mice. **B** – CUR treatment enhanced the capability of BMSC-derived exosomes in restoring the bone mineral density in osteoporotic mice. **C** – CUR treatment enhanced the ability of BMSC-derived exosomes to restore the trabecular number in osteoporotic mice

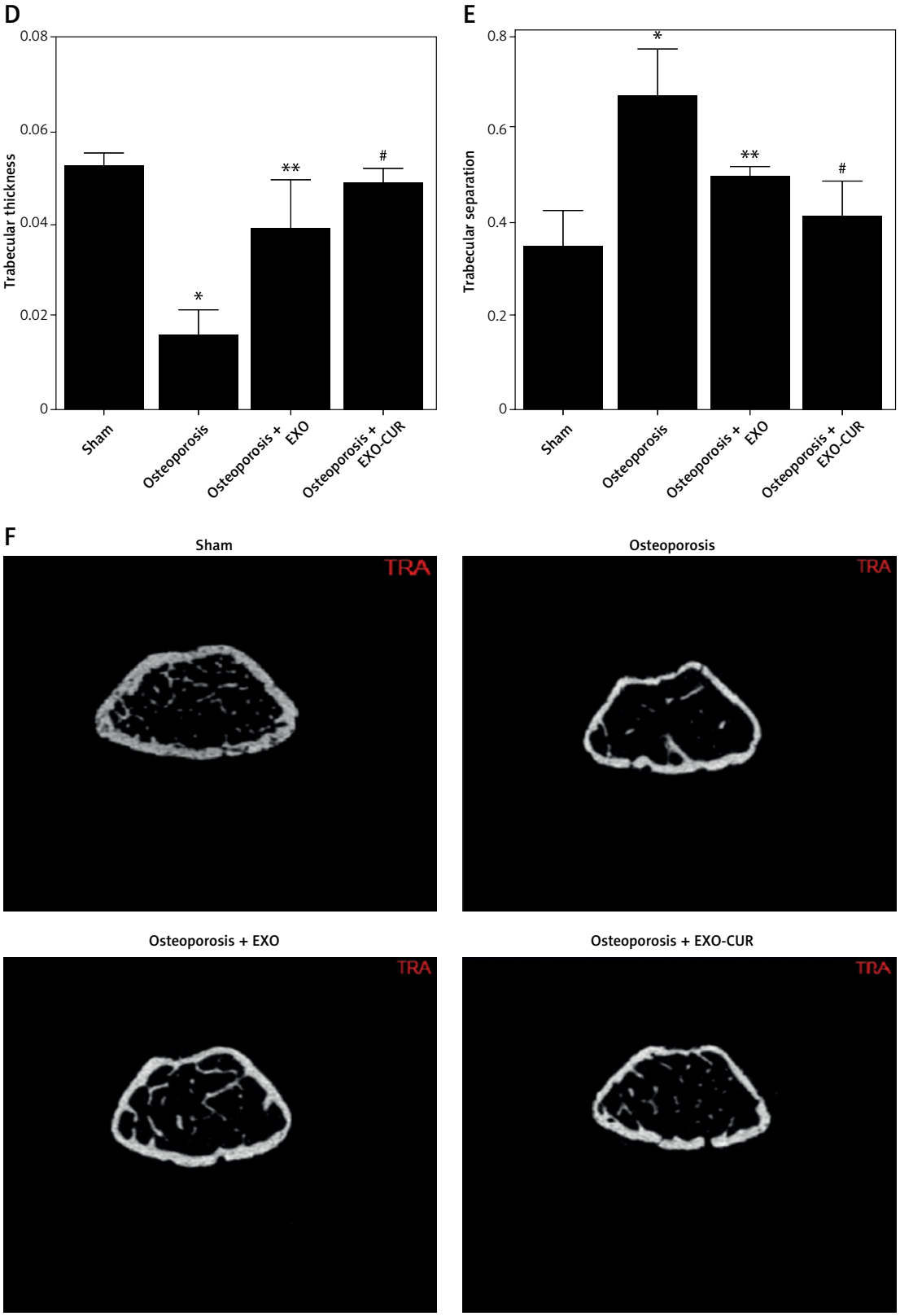

Figure 2. Cont. **D** – CUR treatment enhanced the ability of BMSC-derived exosomes to restore the trabecular thickness in osteoporotic mice. **E** – CUR treatment enhanced the ability of BMSC-derived exosomes to restore the trabecular separation in osteoporotic mice. **F** – Representative micro-CT images of mouse groups

CUR treatment effectively strengthened the capability of BMSC-derived exosomes in maintaining the expression of METTL3, miR-320, and RUNX2 in osteoporotic mice

To examine the molecular mechanism underlying the therapeutic effect of CUR and BMSC-derived exosomes, we performed PCR, Western blot, and immunohistochemistry to analyze the expression of METTL3, RUNX2, and miR-320 in osteoporotic mice treated under different conditions. Accordingly, the expression of METTL3 mRNA and protein was apparently suppressed in osteoporotic mice. Notably, CUR treatment of BMSCs enhanced the ability of BMSC-derived exosomes to maintain the suppressed expression of METTL3 mRNA (Figure 3 A) and protein (Figures 3 B, 4) in osteoporotic mice. In contrast, the activated expression of miR-320 in osteoporotic mice was effectively repressed by the exosomes derived from CUR-treated BMSCs (Figure 3 C). Moreover, the repressed expression of RUNX2 mRNA (Figure 3 D) and protein (Figure 3 E) in osteoporotic mice was effectively maintained by the exosomes derived from CUR-treated BMSCs.

BMSC-derived exosomes markedly enhanced the effect of CUR on regulating the expression of METTL3, miR-320, RUNX2, BGLAP, and LAP in BMSCs

Furthermore, we treated BMSCs with CUR alone or in combination with BMSC-derived exosomes to evaluate their effect on the expression of METTL3, miR-320, RUNX2, BGLAP, and LAP. As shown in

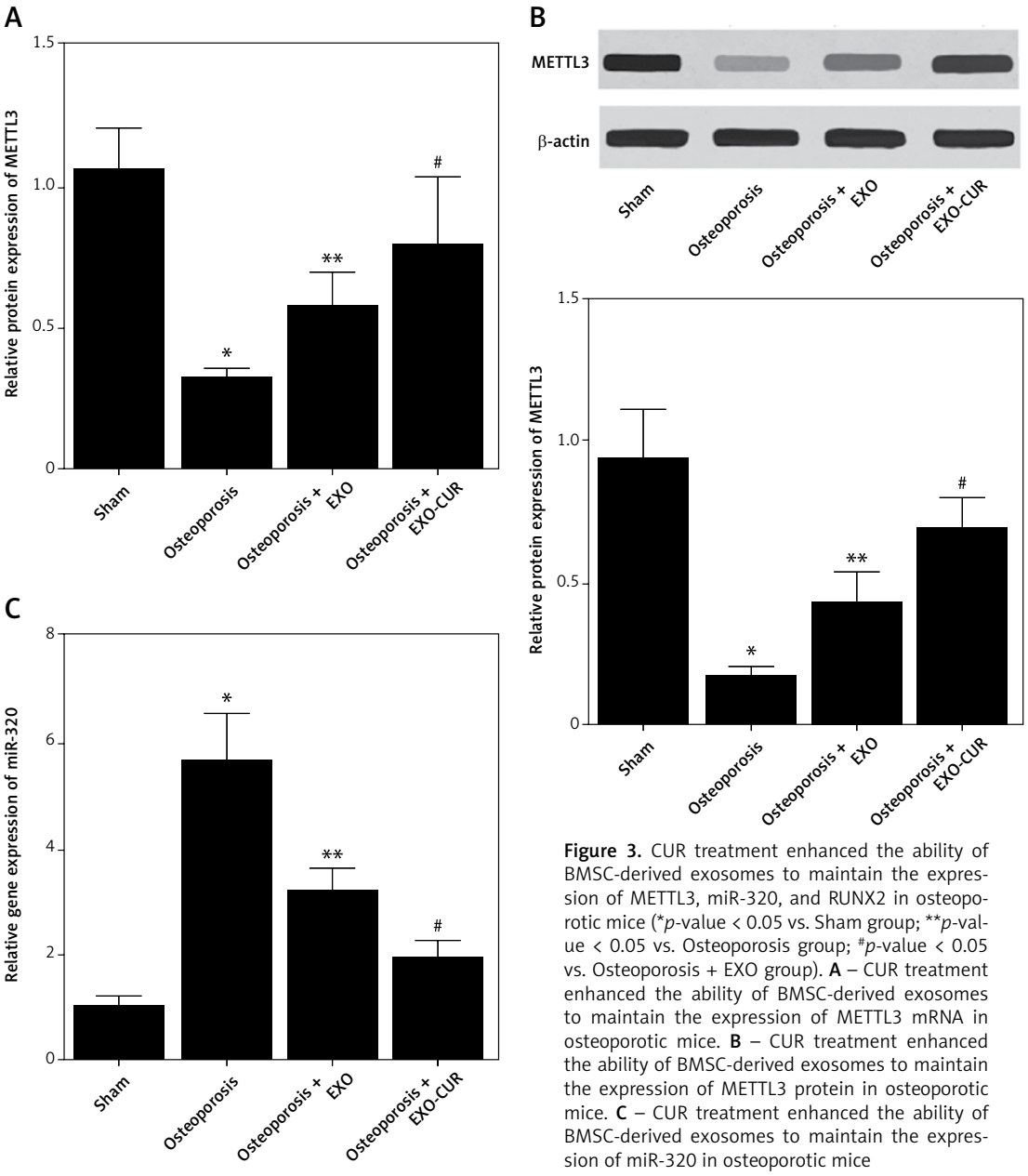

Figure 3. CUR treatment enhanced the ability of BMSC-derived exosomes to maintain the expression of METTL3, miR-320, and RUNX2 in osteoporotic mice (*p-value < 0.05 vs. Sham group; **p-value < 0.05 vs. Osteoporosis group; #p-value < 0.05 vs. Osteoporosis + EXO group). **A** – CUR treatment enhanced the ability of BMSC-derived exosomes to maintain the expression of METTL3 mRNA in osteoporotic mice. **B** – CUR treatment enhanced the ability of BMSC-derived exosomes to maintain the expression of METTL3 protein in osteoporotic mice. **C** – CUR treatment enhanced the ability of BMSC-derived exosomes to maintain the expression of miR-320 in osteoporotic mice

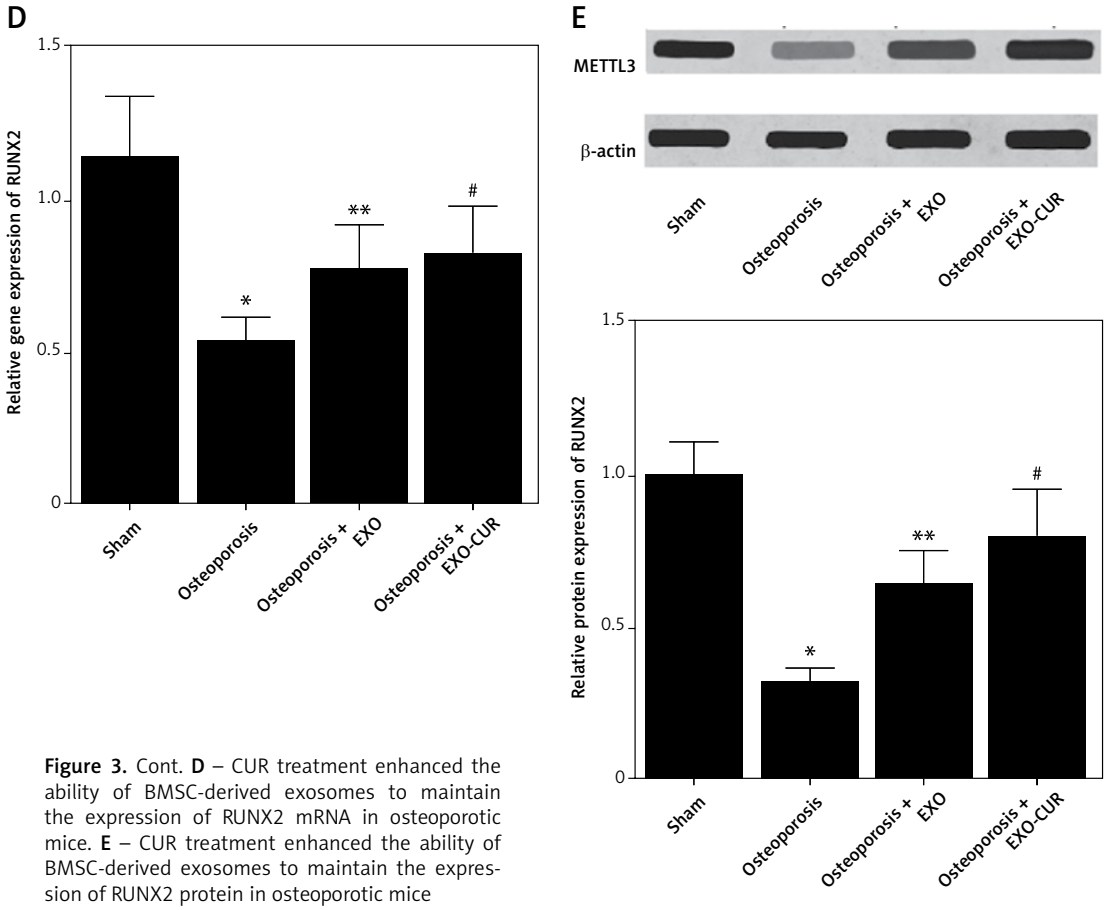

Figure 3. Cont. **D** – CUR treatment enhanced the ability of BMSC-derived exosomes to maintain the expression of RUNX2 mRNA in osteoporotic mice. **E** – CUR treatment enhanced the ability of BMSC-derived exosomes to maintain the expression of RUNX2 protein in osteoporotic mice

Figure 5, BMSC-derived exosomes significantly enhanced the effect of CUR on increasing the expression of METTL3 mRNA (Figure 5 A), METTL3 protein (Figure 5 B), RUNX2 mRNA (Figure 5 D), RUNX2 protein (Figure 5 E), BGLAP mRNA (Figure 5 F) and LAP mRNA (Figure 5 G) as well as on decreasing the expression of miR-320 in BMSCs (Figure 5 C).

METTL3 siRNA notably repressed the expression of METTL3, RUNX2, BGLAP, and LAP, and activated the expression of miR-320 in BMSCs

BMSCs were treated with METTL3 siRNA, and the expression of METTL3, miR-320, RUNX2, BGLAP, and LAP was analyzed using real-time PCR and Western blot. The expression of METTL3 mRNA (Figure 6 A), METTL3 protein (Figure 6 B), RUNX2 mRNA (Figure 6 D), RUNX2 protein (Figure 6 E), BGLAP mRNA (Figure 6 F) and LAP mRNA (Figure 6 G) was evidently suppressed by METTL3 siRNA in BMSCs. The expression of miR-320 was increased in BMSCs treated with METTL3 siRNA (Figure 6 C).

MiR-320 inhibited the expression of RUNX2 through binding to the 3' UTR of RUNX2.

Binding site screening demonstrated that miR-320 could potentially bind to the 3' UTR of RUNX2 (Figure 7 A). Luciferase vectors containing wild type and mutant RUNX2 were established and transfected into BMSCs and MG63 cells along with miR-320. The luciferase activity of wild type RUNX2 vector was significantly inhibited in BMSCs (Figure 7 B) and MG63 (Figure 7 C) cells, indicating that miR-320 suppressed the expression of RUNX2. Moreover, we examined the expression of RUNX2 in BMSCs and MG63 cells treated with different concentrations of a miR-320 precursor. The expression of RUNX2 mRNA was significantly reduced in miR-320-treated BMSCs (Figure 7 D) and MG63 (Figure 7 E) cells.

In summary, our study demonstrated that BMSC-derived exosomes and CUR jointly enhanced the expression of METTL3, which downregulated the expression of miR-320, resulting in the upregulation of RUNX2. As a result, osteogenic differentiation was enhanced to alleviate osteoporosis (Figure 8).

Discussion

In this study, we harvested exosomes from bone marrow stem cells and treated osteoporotic mice with the combination of CUR and BMSC-derived exosomes. The therapeutic effect of CUR on osteoporosis was markedly elevated by

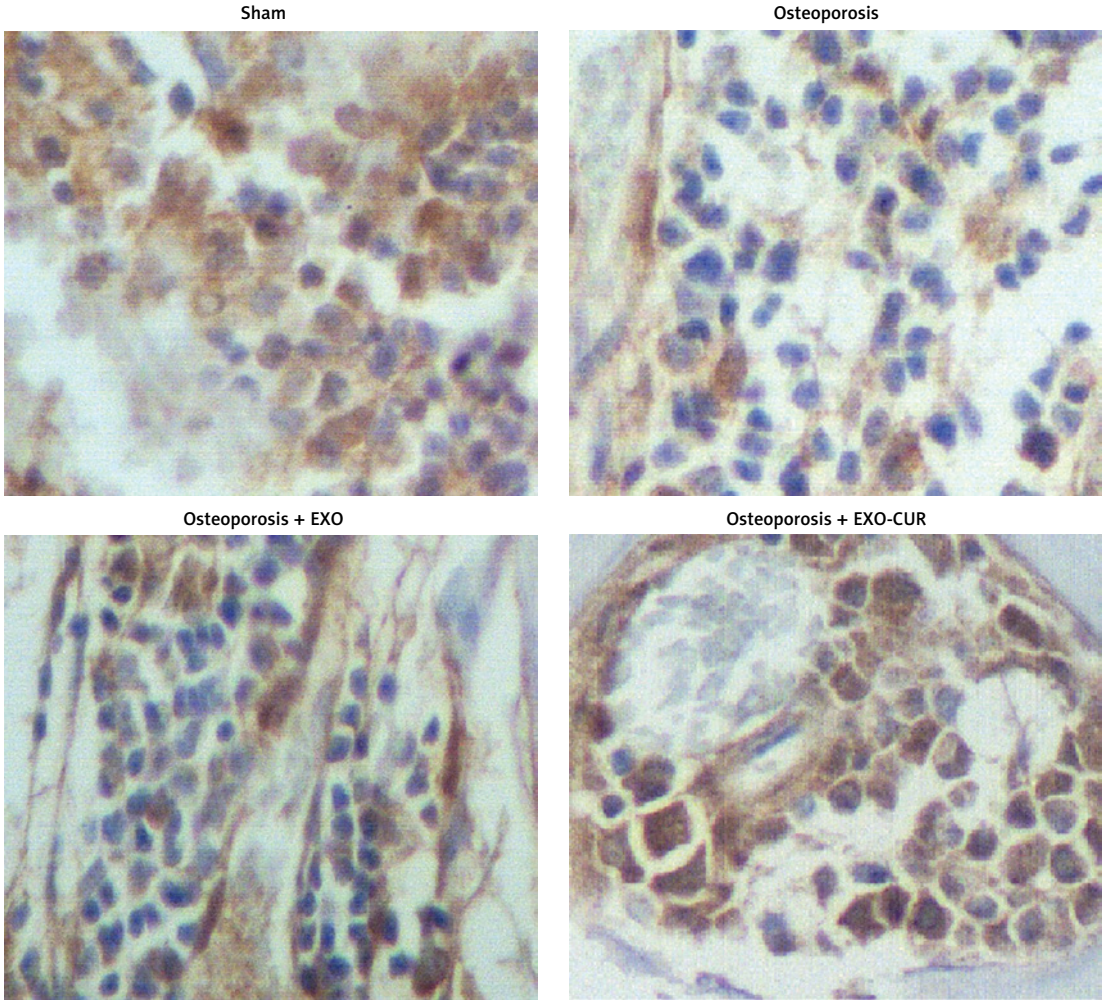

Figure 4. Immunohistochemistry analysis showed that CUR treatment enhanced the ability of BMSC-derived exosomes to maintain the expression of METTL3 protein in osteoporotic mice

BMSC-derived exosomes. In addition, we performed real-time PCR, Western blot and IHC to examine the expression of METTL3, miR-320, and RUNX2 at both the mRNA and protein levels in osteoporotic mice treated under different conditions. BMSC-derived exosomes strengthened with CUR significantly restored the expression of METTL3, miR-320 and RUNX2 in osteoporotic mice. As a phenolic substance obtained from *Curcuma longa*, CUR exhibits certain anti-inflammatory, anti-tumor, and anti-mutagenic effects [28, 29]. Studies have suggested that CUR affects both fat accumulation and bone health in the body. In addition, CUR may cause the apoptosis of osteoclasts while preventing the growth of osteoclasts by decreasing RANKL expression in BMSCs [29, 30]. It was also found that CUR reduced *in vivo* osteoporosis induced by DXM [31].

It was reported that BMSC proliferation on modified surfaces of LC was significantly increased by 0.05 mg/ml of BMP2. Similarly, osteonectin expression was increased by BMP2 on LC as well as UDMA surfaces [32]. Surprisingly, a recent study suggested that the accumulation of m6A in both mice and humans was regulated by mRNAs through their selective binding to METTL3 [13, 33]. Consistently, Vashisht *et al.* recently suggested that CUR loaded in exosomes is not only resistant to enzymatic digestion, but also shows elevated permeability in the digestive tract [26, 34, 35]. Certain evidence suggested that MSC-derived exosomes as well as exosome-like nanoparticles derived from edible plants can also resist enzymatic digestion [26, 36].

A previous study suggested that exosomal MALAT1 in BMSCs may contribute to increased osteogenic activity as well as relief of osteoporosis symptoms through functioning as a sponge of miR-34c to upregulate the expression of SATB2 [37]. Also, it was found that nearly 75% of super-enhancer RNAs (seRNAs) exhibit m6A modification peaks. In addition, the level of m6A methylation in seRNAs was decreased in Mettl3 KO models [38]. Furthermore, pre-miR-320 methylation in the nucleus results in the downregulation of miR-320 expression in the cytoplasm, contributing to the

osteogenic potential of METTL3 [19]. Additionally, the downregulation of miR-320 rescued the bone mass loss shown in METTL3$^{+/-}$ knockout [23]. In this study, we treated BMSCs with CUR alone or in combination with BMSC-derived exosomes. BMSC-derived exosomes significantly enhanced the role of CUR in promoting the expression of METTL3 and RUNX2 mRNA and in suppressing the expression of miR-320 in BMSCs.

Bioinformatics studies showed that the 3'-UTR of RUNX2 contains four miR-320 binding sites. The interaction of RUNX2 3'-UTR and miR-320 is also specific, as mutations in the 3'-UTR of RUNX2 blocked the binding between miR-320 and RUNX2 3'-UTR [39]. In this study, we performed a luciferase assay to explore the inhibitory role of miR-320 in the expression of RUNX2. The luciferase activity of wild type RUNX2 was

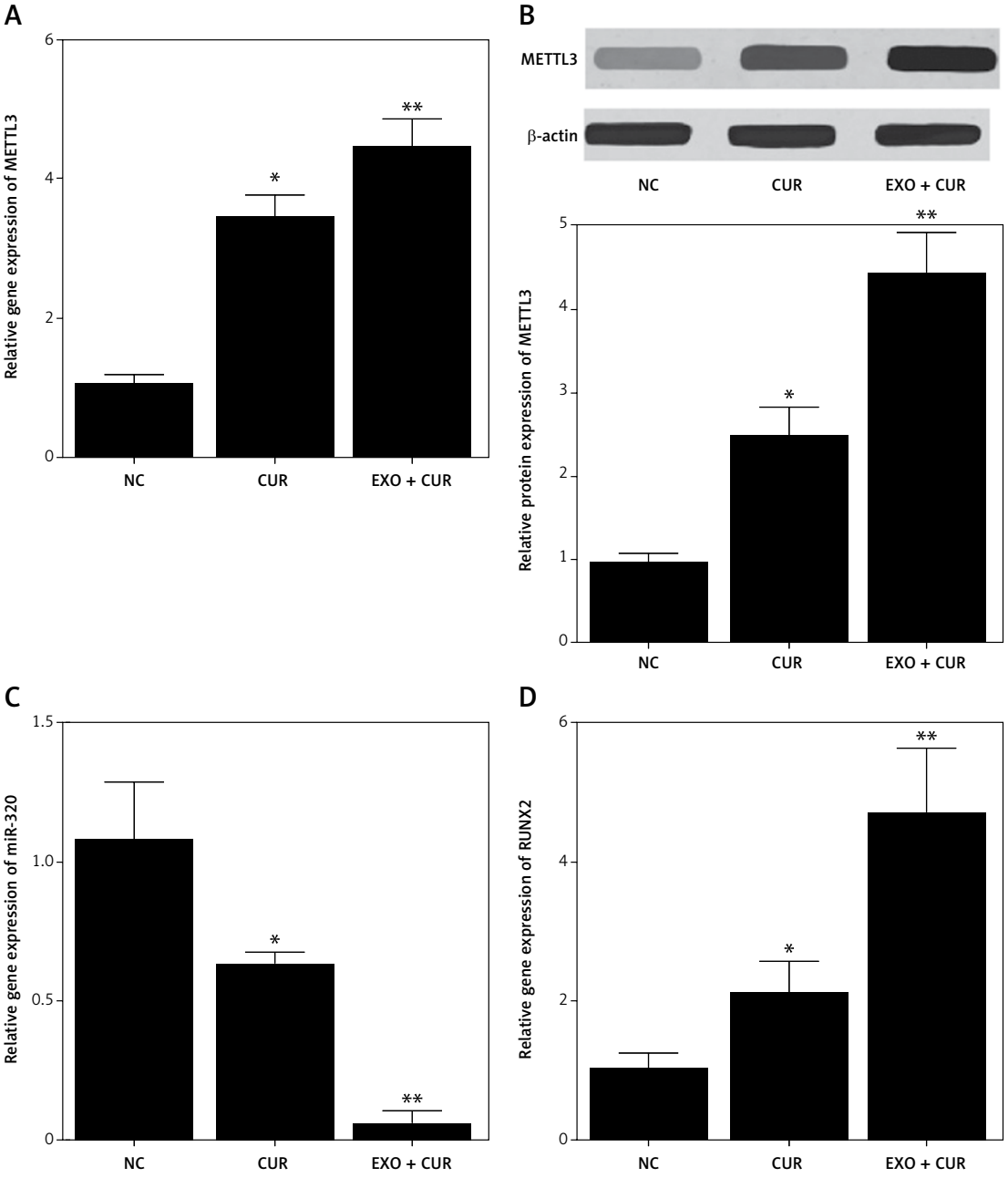

Figure 5. Exosomes derived from CUR-treated BMSCs strengthened the ability of CUR to alter the expression of METTL3, miR-320, RUNX2, BGLAP, and LAP in BMSCs (*p-value < 0.05 vs. NC group; **p-value < 0.05 vs. CUR group). **A** – Exosomes derived from CUR-treated BMSCs strengthened the effect of CUR in promoting the expression of METTL3 mRNA in BMSCs. **B** – Exosomes derived from CUR-treated BMSCs strengthened the effect of CUR in promoting the expression of METTL3 protein in BMSCs. **C** – Exosomes derived from CUR-treated BMSCs strengthened the effect of CUR in suppressing the expression of miR-320 in BMSCs. **D** – Exosomes derived from CUR-treated BMSCs strengthened the effect of CUR in promoting the expression of RUNX2 mRNA in BMSCs

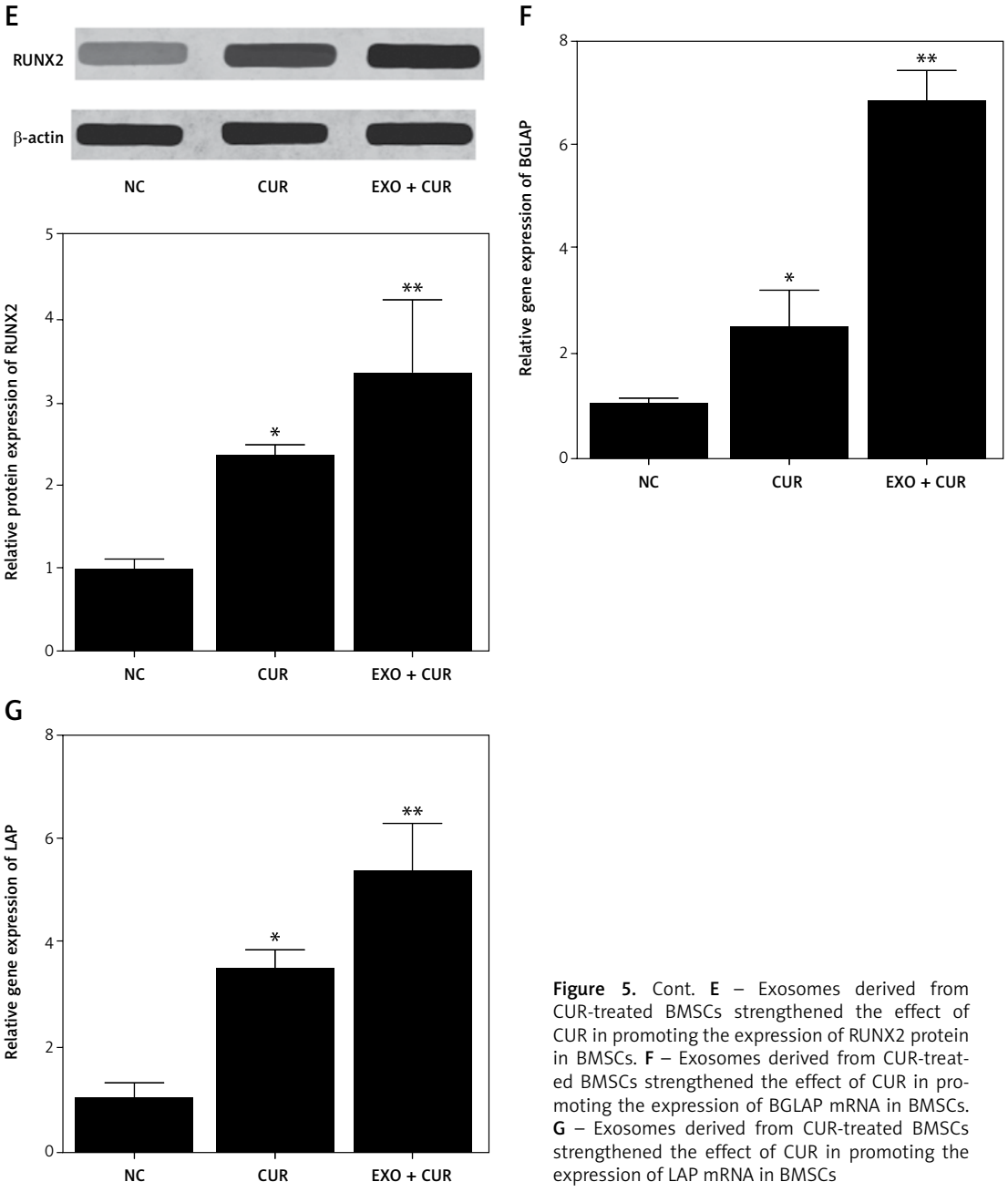

Figure 5. Cont. **E** – Exosomes derived from CUR-treated BMSCs strengthened the effect of CUR in promoting the expression of RUNX2 protein in BMSCs. **F** – Exosomes derived from CUR-treated BMSCs strengthened the effect of CUR in promoting the expression of BGLAP mRNA in BMSCs. **G** – Exosomes derived from CUR-treated BMSCs strengthened the effect of CUR in promoting the expression of LAP mRNA in BMSCs

significantly repressed by miR-320 in BMSCs and MG63 cells.

RUNX2 belongs to the family of RUNT related transcription factors that are essential in the course of skeletal development during embryogenesis. RUNX2 is also recognized for its oncogenic functions. In fact, numerous studies revealed that the dysregulation of RUNX2 leads to tumor progression as well as tumor invasion [40]. Additionally, RUNX2 was found to be involved in bone development as well as hypertrophic differentiation of chondrocytes [41, 42]. Past studies showed that the adipocytic differentiation of MSCs was inhibited by RUNX2 [43]. It was also shown that the differentiation of MSCs into osteoblasts is the main pathway for bone formation [39]. Runx2 can activate and regulate osteogenesis via many different signaling pathways, such as the TGF-β1, BMP, Wnt, Hedgehog, and NELL-1 signaling pathways [26, 27]. Mice carrying the homozygous $Runx2^{-/-}$ mutations lack differentiated osteoblasts upon birth [44, 45]. While Runx2 does not act as a crucial regulator in the differentiation of adipocytes, its role in enhancing osteogenesis may affect the differentiation of adipocyte lineages [46]. In addition, we treated BMSCs with METTL3 siRNA and analyzed the expression of METTL3, miR-320, RUNX2, BGLAP and LAP in BMSCs. The expression of METTL3, RUNX2, BGLAP, and LAP was significantly suppressed by METTL3 siRNA, while the

expression of miR-320 was significantly enhanced by METTL3 siRNA in BMSCs.

However, our study is limited by the lack of clinical validation. Although our findings suggest that exosomes derived from CUR-treated BMSCs could promote the therapeutic effect of CUR, future clinical validation should be conducted.

In conclusion, our study demonstrated that BMSC-derived exosomes could modulate the signaling pathway of METTL3/miRNA-320/RUNX2 to attenuate osteoporosis by promoting osteogenic differentiation of BMSCs. Moreover, exosomes derived from CUR-treated BMSCs promoted the therapeutic effect of CUR.

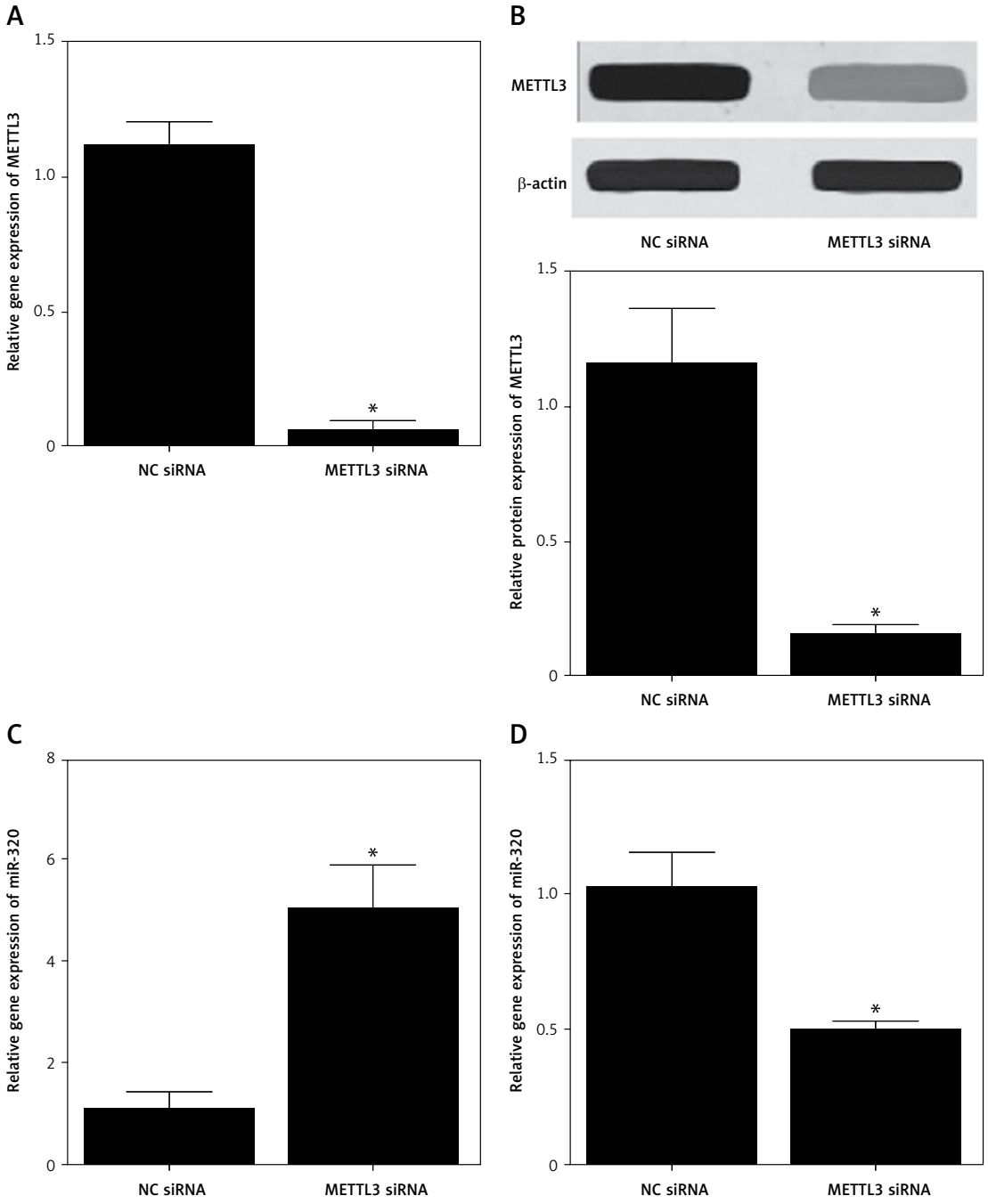

Figure 6. METTL3 siRNA transfection altered the expression of METTL3, miR-320, RUNX2, BGLAP, and LAP in BMSCs (*p-value < 0.05 vs. NC siRNA group). **A** – Expression of METTL3 mRNA was suppressed by METTL3 siRNA in BMSCs. **B** – Expression of METTL3 protein was suppressed by METTL3 siRNA in BMSCs. **C** – Expression of miR-320 was increased by METTL3 siRNA in BMSCs. **D** – Expression of RUNX2 mRNA was suppressed by METTL3 siRNA in BMSCs

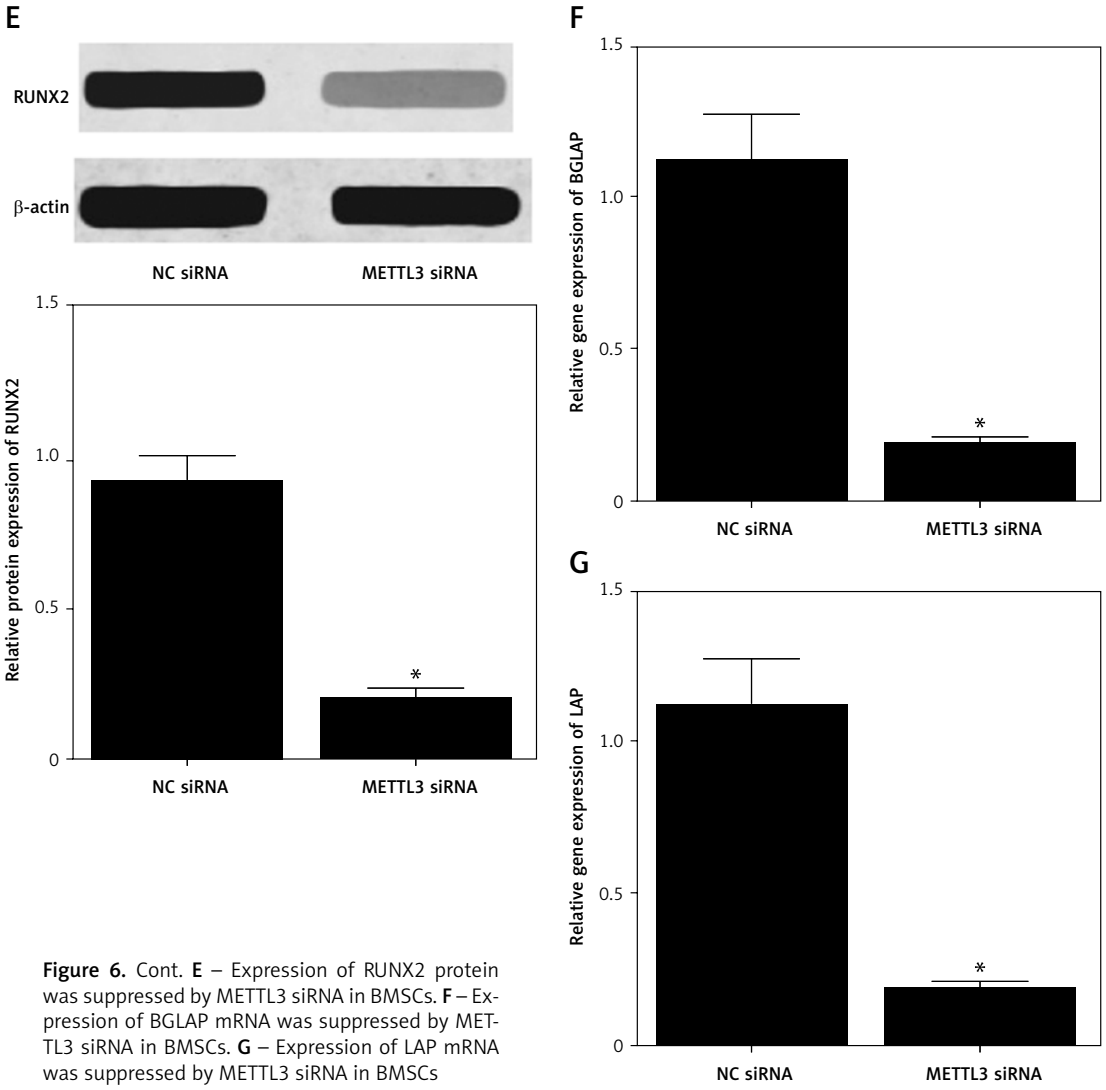

Figure 6. Cont. **E** – Expression of RUNX2 protein was suppressed by METTL3 siRNA in BMSCs. **F** – Expression of BGLAP mRNA was suppressed by METTL3 siRNA in BMSCs. **G** – Expression of LAP mRNA was suppressed by METTL3 siRNA in BMSCs

Funding

No external funding.

Ethical approval

Not applicable.

Conflict of interest

The author declares no conflict of interest.

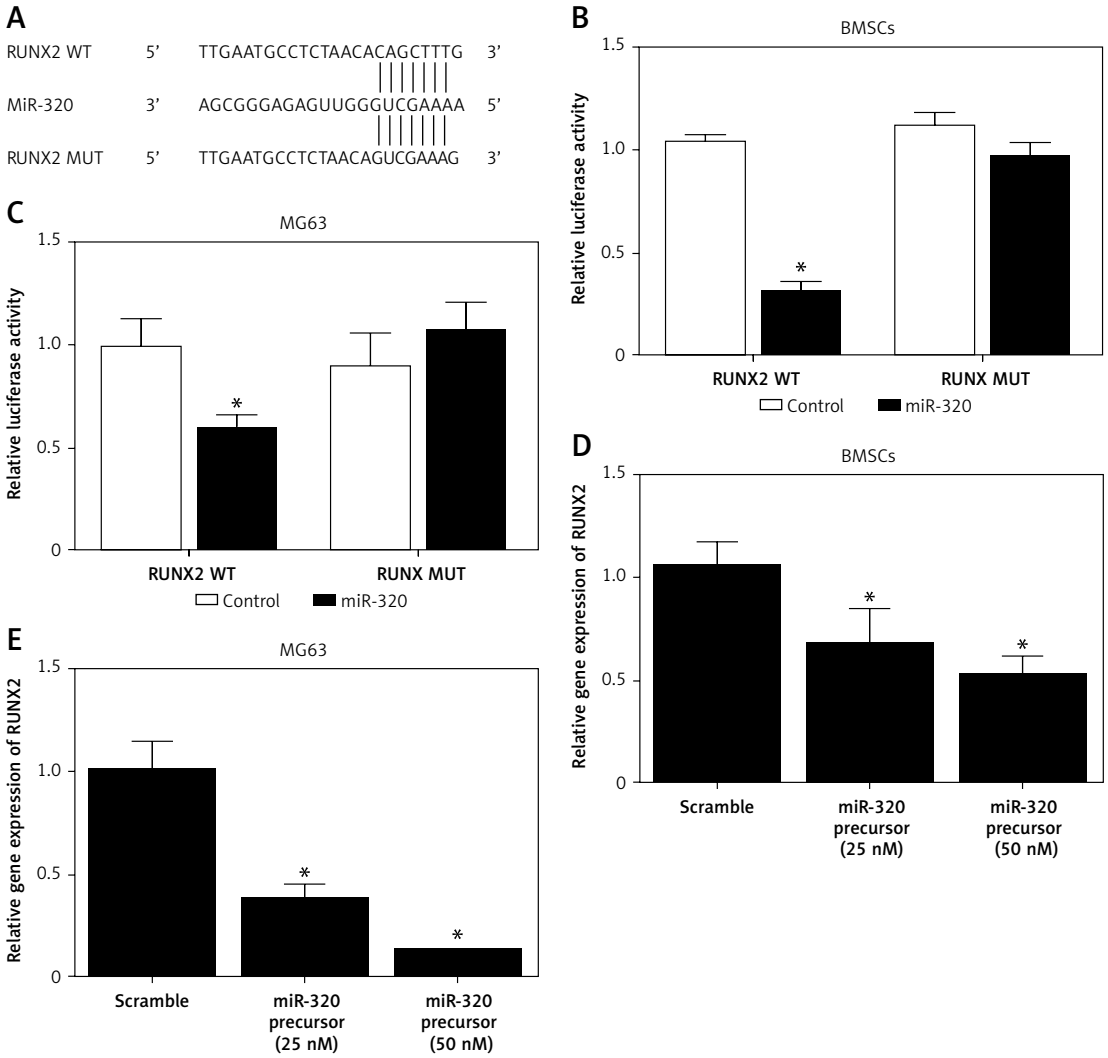

Figure 7. MiR-320 suppressed the expression of RUNX2 through binding to its 3' UTR. **A** – Sequence analysis indicated that miR-320 could potentially bind to the 3' UTR of RUNX2. **B** – Luciferase activity of wild type RUNX2 was markedly suppressed by miR-320 in BMSCs (**p*-value < 0.05 vs. control group). **C** – Luciferase activity of wild type RUNX2 was markedly suppressed by miR-320 in MG63 cells (**p*-value < 0.05 vs. control group). **D** – Expression of RUNX2 mRNA was repressed by miR-320 precursors in a dose-dependent manner in BMSCs (**p*-value < 0.05 vs. scramble group). **E** – Expression of RUNX2 mRNA was repressed by miR-320 precursors in a dose-dependent manner in MG63 cells (**p*-value < 0.05 vs. scramble group)

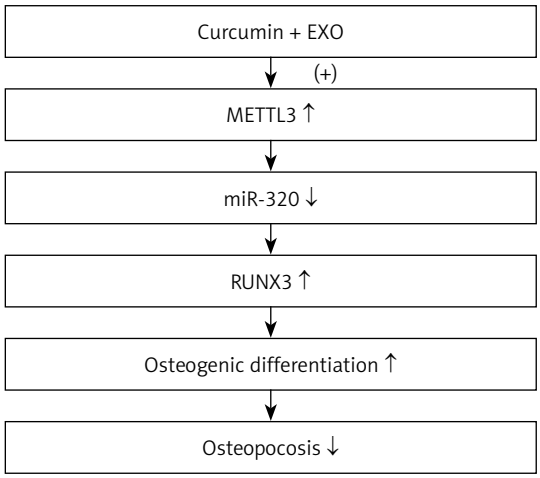

Figure 8. Schematic illustration of the study

References

1. Pietschmann P, Rauner M, Sipos W, Kerschan-Schindl K. Osteoporosis: an age-related and gender-specific disease--a mini-review. Gerontology 2009; 55: 3-12.
2. Mulder JE, Kolatkar NS, LeBoff MS. Drug insight: Existing and emerging therapies for osteoporosis. Nat Clin Pract Endocrinol Metab 2006; 2: 670-80.
3. Burge R, Dawson-Hughes B, Solomon DH, Wong JB, King A, Tosteson A. Incidence and economic burden of osteoporosis-related fractures in the United States, 2005-2025. J Bone Miner Res 2007; 22: 465-75.
4. Toden S, Theiss AL, Wang X, Goel A. Essential turmeric oils enhance anti-inflammatory efficacy of curcumin in dextran sulfate sodium-induced colitis. Sci Rep 2017; 7: 814.
5. Shlar I, Droby S, Rodov V. Modes of antibacterial action of curcumin under dark and light conditions: a toxicoproteomics approach. J Proteomics 2017; 160: 8-20.
6. Mollazadeh H, Cicero AFG, Blesso CN, Pirro M, Majeed M, Sahebkar A. Immune modulation by curcumin: the role of interleukin-10. Crit Rev Food Sci Nutr 2019; 59: 89-101.
7. Pan CJ, Tang JJ, Shao ZY, Wang J, Huang N. Improved blood compatibility of rapamycin-eluting stent by incorporating curcumin. Colloids Surf B Biointerfaces 2007; 59: 105-11.
8. Mawani Y, Orvig C. Improved separation of the curcuminoids, syntheses of their rare earth complexes, and studies of potential antiosteoporotic activity. J Inorg Biochem 2014; 132: 52-8.
9. Khanizadeh F, Rahmani A, Asadollahi K, Ahmadi MRH. Combination therapy of curcumin and alendronate modulates bone turnover markers and enhances bone mineral density in postmenopausal women with osteoporosis. Arch Endocrinol Metab 2018; 62: 438-45.
10. Ahmed MF, El-Sayed AK, Chen H, et al. Comparison between curcumin and all-trans retinoic acid in the osteogenic differentiation of mouse bone marrow mesenchymal stem cells. Exp Ther Med 2019; 17: 4154-66.
11. Wang H, Zhang Y, Yang Y, et al. Curcumin pretreatment protects against hypoxia/reoxgenation injury via improvement of mitochondrial function, destabilization of HIF-1α and activation of Epac1-Akt pathway in rat bone marrow mesenchymal stem cells. Biomed Pharmacother 2019; 109: 1268-75.
12. Sahebkar A, Cicero AFG, Simental-Mendía LE, Aggarwal BB, Gupta SC. Curcumin downregulates human tumor necrosis factor-α levels: a systematic review and meta-analysis of randomized controlled trials. Pharmacol Res 2016; 107: 234-42.
13. Lu N, Li X, Yu J, et al. Curcumin attenuates lipopolysaccharide-induced hepatic lipid metabolism disorder by modification of m(6) A RNA methylation in piglets. Lipids 2018; 53: 53-63.
14. Xie Y, Zhao X, Jia H, Ma B. Derivation and characterization of goat fetal fibroblast cells induced with human telomerase reverse transcriptase. In Vitro Cell Dev Biol Anim 2013; 49: 8-14.
15. Timmers L, Lim SK, Arslan F, et al. Reduction of myocardial infarct size by human mesenchymal stem cell conditioned medium. Stem Cell Res 2007; 1: 129-37.
16. Ebrahim N, Ahmed IA, Hussien NI, et al. Mesenchymal stem cell-derived exosomes ameliorated diabetic nephropathy by autophagy induction through the mTOR signaling pathway. Cells 2018; 7: 226.
17. Furuta T, Miyaki S, Ishitobi H, et al. Mesenchymal stem cell-derived exosomes promote fracture healing in a mouse model. Stem Cells Transl Med 2016; 5: 1620-30.
18. Katsuda T, Ochiya T. Molecular signatures of mesenchymal stem cell-derived extracellular vesicle-mediated tissue repair. Stem Cell Res Ther 2015; 6: 212.
19. Zhao P, Xiao L, Peng J, Qian YQ, Huang CC. Exosomes derived from bone marrow mesenchymal stem cells improve osteoporosis through promoting osteoblast proliferation via MAPK pathway. Eur Rev Med Pharmacol Sci 2018; 22: 3962-70.
20. Visvanathan A, Patil V, Arora A, et al. Essential role of METTL3-mediated m(6)A modification in glioma stem-like cells maintenance and radioresistance. Oncogene 2018; 37: 522-33.
21. Wen J, Lv R, Ma H, et al. Zc3h13 Regulates nuclear RNA m(6)A methylation and mouse embryonic stem cell self-renewal. Mol Cell 2018; 69: 1028-38e6.
22. Wu Y, Xie L, Wang M, et al. Mettl3-mediated m(6)A RNA methylation regulates the fate of bone marrow mesenchymal stem cells and osteoporosis. Nat Commun 2018; 9: 4772.
23. Yan G, Yuan Y, He M, et al. m(6)A methylation of precursor-miR-320/RUNX2 controls osteogenic potential of bone marrow-derived mesenchymal stem cells. Mol Ther Nucleic Acids 2020; 19: 421-36.
24. Komori T. Regulation of osteoblast differentiation by Runx2. Adv Exp Med Biol 2010; 658: 43-9.
25. Pratap J, Wixted JJ, Gaur T, et al. Runx2 transcriptional activation of Indian Hedgehog and a downstream bone metastatic pathway in breast cancer cells. Cancer Res 2008; 68: 7795-802.
26. Vashisht M, Rani P, Onteru SK, Singh D. Curcumin encapsulated in milk exosomes resists human digestion and possesses enhanced intestinal permeability in vitro. Appl Biochem Biotechnol 2017; 183: 993-1007.
27. Oskouie MN, Moghaddam NSA, Butler AE, Zamani P, Sahebkar A. Therapeutic use of curcumin-encapsulated and curcumin-primed exosomes. J Cell Physiol 2019; 234: 8182-91.
28. Aggarwal BB, Sundaram C, Malani N, Ichikawa H. Curcumin: the Indian solid gold. Adv Exp Med Biol 2007; 595: 1-75.
29. Bharti AC, Takada Y, Aggarwal BB. Curcumin (diferuloylmethane) inhibits receptor activator of NF-kappa B ligand-induced NF-kappa B activation in osteoclast precursors and suppresses osteoclastogenesis. J Immunol 2004; 172: 5940-7.
30. Ozaki K, Kawata Y, Amano S, Hanazawa S. Stimulatory effect of curcumin on osteoclast apoptosis. Biochem Pharmacol 2000; 59: 1577-81.
31. Chen Z, Xue J, Shen T, Mu S, Fu Q. Curcumin alleviates glucocorticoid-induced osteoporosis through the regulation of the Wnt signaling pathway. Int J Mol Med 2016; 37: 329-38.
32. Böhrnsen F, Krier M, Grohmann S, et al. MSC differentiation on two-photon polymerized, stiffness and BMP2 modified biological copolymers. Biomed Mater 2019; 14: 035001.
33. Chen T, Hao YJ, Zhang Y, et al. m(6)A RNA methylation is regulated by microRNAs and promotes reprogramming to pluripotency. Cell Stem Cell 2015; 16: 289-301.
34. Liao Y, Du X, Li J, Lönnerdal B. Human milk exosomes and their microRNAs survive digestion in vitro and are taken up by human intestinal cells. Mol Nutr Food Res 2017; 61: doi: 10.1002/mnfr.201700082.
35. Ma H, Xu Y, Zhang R, Guo B, Zhang S, Zhang X. Differential expression study of circular RNAs in exosomes from serum and urine in patients with idiopathic membranous nephropathy. Arch Med Sci 2019; 15: 738-53.

36. Agrawal AK, Aqil F, Jeyabalan J, et al. Milk-derived exosomes for oral delivery of paclitaxel. Nanomedicine 2017; 13: 1627-36.
37. Yang X, Yang J, lei P, Wen T. LncRNA MALAT1 shuttled by bone marrow-derived mesenchymal stem cells-secreted exosomes alleviates osteoporosis through mediating microRNA-34c/SATB2 axis. Aging 2019; 11: 8777-91.
38. Liu J, Dou X, Chen C, et al. N (6)-methyladenosine of chromosome-associated regulatory RNA regulates chromatin state and transcription. Science 2020; 367: 580-6.
39. Hamam D, Ali D, Vishnubalaji R, et al. microRNA-320/RUNX2 axis regulates adipocytic differentiation of human mesenchymal (skeletal) stem cells. Cell Death Dis 2014; 5: e1499.
40. Sancisi V, Manzotti G, Gugnoni M, et al. RUNX2 expression in thyroid and breast cancer requires the cooperation of three non-redundant enhancers under the control of BRD4 and c-JUN. Nucleic Acids Res 2017; 45: 11249-67.
41. Yu S, Geng Q, Sun F, Yu Y, Pan Q, Hong A. Osteogenic differentiation of C2C12 myogenic progenitor cells requires the Fos-related antigen Fra-1 – a novel target of Runx2. Biochem Biophys Res Commun 2013; 430: 173-8.
42. Li H, Xie H, Liu W, et al. A novel microRNA targeting HDAC5 regulates osteoblast differentiation in mice and contributes to primary osteoporosis in humans. J Clin Invest 2009; 119: 3666-77.
43. Kobayashi H, Gao YH, Ueta C, Yamaguchi A, Komori T. Multilineage differentiation of Cbfa1-deficient calvarial cells in vitro. Biochem Biophys Res Commun 2000; 273: 630-6.
44. Otto F, Thornell AP, Crompton T, et al. Cbfa1, a candidate gene for cleidocranial dysplasia syndrome, is essential for osteoblast differentiation and bone development. Cell 1997; 89: 765-71.
45. Hesse E, Saito H, Kiviranta R, et al. Zfp521 controls bone mass by HDAC3-dependent attenuation of Runx2 activity. J Cell Biol 2010; 191: 1271-83.
46. James AW. Review of signaling pathways governing msc osteogenic and adipogenic differentiation. Scientifica 2013; 2013: 684736.